# Multimodality Screening of Hepatic Nodules in Patients With Congenital Heart Disease After Fontan Procedure: Role of Ultrasound, ARFI Elastography, CT, and MRI

Natally Horvat[1]
Manoel Souza Rocha[1]
Aline Lopes Chagas[2]
Brunna Clemente Oliveira[1]
Mariana Poltronieri Pacheco[2]
Maria Angélica Binotto[3]
Nana Miura Ikari[3]
Denise Cerqueira Paranaguá-Vezozzo[2]
Hilton Muniz Leao-Filho[1]
João Rafael Terneira Vicentini[1]
Mauricio Ricardo Moreira da Silva Filho[4]
Marcelo Biscegli Jatene[3]
Flair José Carrilho[2]
Giovanni Guido Cerri[1]

**Keywords:** CT, Fontan procedure, liver disease, MDCT, MRI, ultrasound

doi.org/10.2214/AJR.18.19762

Received February 25, 2018; accepted after revision May 9, 2018.

[1]Radiology Department, Hospital das Clínicas da Faculdade de Medicina da Universidade de São Paulo, Dr. Enéas de Carvalho Aguiar, Rua Dr. Ovídio Pires de Campos, 255 Cerqueira César, São Paulo, SP 05403-900, Brazil. Address correspondence to N. Horvat (natallymhorvat@gmail.com).

[2]Hepatology Department, Hospital das Clínicas da Faculdade de Medicina da Universidade de São Paulo, São Paulo, Brazil.

[3]Cardiology Department, Hospital das Clínicas da Faculdade de Medicina da Universidade de São Paulo, São Paulo, Brazil.

[4]Medical School, Universidade de São Paulo, São Paulo, Brazil.

*AJR* 2018; 211:1212–1220

0361–803X/18/2116–1212



**OBJECTIVE.** Currently, there is no consensus in the literature regarding the screening of hepatic nodules in patients who have undergone the Fontan procedure. The objectives of this study are to evaluate in this population the frequency of hepatic nodules at ultrasound (US), CT, and MRI; to measure liver stiffness using acoustic radiation force impulse (ARFI) elastography; and to investigate predictive factors for hepatic nodules.

**SUBJECTS AND METHODS.** In this cross-sectional study, 49 patients who underwent the Fontan procedure were prospectively recruited from August 2014 through June 2016. These patients underwent clinical evaluation for hepatic disorders, ARFI elastography, US, CT, and MRI.

**RESULTS.** Most of the patients had no symptoms, and hepatic nodules were detected in three of 49 (6.1%) patients at US, 14 of 44 (31.8%) patients at CT, and 19 of 48 (39.6%) patients at MRI. Liver stiffness at ARFI elastography was significantly higher in patients with hepatic nodules than in patients without such nodules (2.64 ± 0.81 m/s vs 1.94 ± 0.49 m/s; $p = 0.002$) and was a significant predictor of hepatic nodule (AUC, 0.767; $p = 0.002$). No clinical or laboratory data had any significant correlation with the existence of hepatic nodules, including time since Fontan procedure.

**CONCLUSION.** In our study, more than one-third of patients had hepatic nodules at CT or MRI, but US did not detect most hepatic nodules. Liver stiffness at ARFI elastography was significantly higher in patients with hepatic nodules, and it may help guiding which patient should be further imaged with CT or MRI.

The Fontan procedure is a cardiac palliative surgery described in 1971 by Fontan and Baudet [1] and represents 3.2% of all congenital cardiac operations [2]. It is indicated to treat patients with congenital heart disease characterized by a single functional ventricle [1, 3]. In the Fontan procedure, staged palliation surgeries are made to reroute the systemic venous return directly into the pulmonary circulation, bypassing the subpulmonary ventricle and restoring normal saturation to these patients [4] (Fig. 1). The Fontan procedure has evolved, allowing such patients to reach adulthood, but with significant systemic consequences, particularly to the liver [5–7].

Fontan liver disease is multifactorial and may result from both pre– and post–Fontan procedure liver damage [8, 9]. Some studies have found that the elevated systemic pressure after the Fontan procedure is transmitted to the hepatic perivenular areas and results in portal deprivation [9, 10]. Consequently, it increases the arterial flow by the hepatic arterial buffer response [11] and increases intrahepatic markers of inflammation, angiogenesis, proliferation, and fibrosis [9], which were also observed in an experimental model of portal deprivation [12]. Furthermore, patients who have undergone the Fontan procedure also show reduced dynamic cardiac output with hypoxia in either pre– and post–Fontan operation, increasing the hepatic injury. The association of those factors causes liver fibrosis, cirrhosis with or without portal hypertension, and hepatic nodules, which are frequently benign, mainly regenerative, nodules; however, hepatocellular carcinoma (HCC) has been increasingly reported and it is difficult to differentiate from benign nodules [10, 13–20].

Currently, there is no consensus in the literature regarding liver evaluation in patients after the Fontan procedure, particularly on the screening of hepatic nodule, when to start the screening, and which is the best imaging mo-

dality indicated for it. The American Heart Association [21] and the Canadian Cardiovascular Society [22] consensus statements discuss each imaging modality, laboratory test, and liver biopsy, but the final recommendation is serial evaluation of liver function without a specific recommendation regarding imaging examinations. The American College of Cardiology recommends ultrasound (US) and laboratory testing [23]. On the other hand, the European Society of Cardiology describes that hepatic evaluation by US and CT is important, without a precise recommendation [24]. With regard to the evaluation of hepatic fibrosis or cirrhosis, liver biopsy remains the reference standard, but it is an invasive method and is susceptible to sample error [25]. The risk of bleeding is particularly relevant in this population, considering that anticoagulants are commonly used to prevent thromboembolic events. In this context, noninvasive modalities have emerged to estimate the degree of fibrosis on the basis of laboratory tests and imaging modalities, including acoustic radiation force impulse (ARFI) elastography [26]. Up to now, to our knowledge, there is no study that compared US, CT, and MRI in the evaluation of hepatic nodules in patients after the Fontan procedure.

In this scenario, the purposes of this study were to evaluate the frequency of hepatic nodules at US, CT, and MRI in patients after the Fontan procedure; to measure the liver stiffness using ARFI elastography; and to investigate possible predictive factors for hepatic nodules.

## Subjects and Methods

### *Study Population*

In this single-center cross-sectional study, patients who had undergone the Fontan procedure were consecutively recruited from our cardiology department from August 2014 to June 2016. The study protocol was approved by the institutional review board, and informed written consent was obtained from each subject. The inclusion criteria were age older than 18 years and at least 5 years elapsed since the Fontan procedure. The exclusion criteria were pregnancy and patients who could not undergo either CT or MRI. The final study population was 49 patients.

These patients underwent hepatology evaluation and radiologic liver examination, including upper abdominal US, liver ARFI elastography, upper abdomen triple-phase CT, and gadoxetic acid–enhanced MRI, on the same day. The cardiologic data were retrospectively reviewed. One patient did not undergo ARFI elastography because of ascites, five patients did not undergo CT owing to a history of contrast media allergic reaction, and one patient did not undergo MRI because of a cardiac pacemaker.

### *Cardiologic Data*

Cardiologic data were obtained from a detailed medical record review made by two cardiologists with 30 and 28 years of experience in the Fontan procedure using a standardized form.

### *Hepatologic Examination*

All patients were evaluated by two hepatologists with 10 and 5 years of experience in hepatology who performed a full history and physical examination related to liver disease.

### *Laboratory Studies*

Patients had blood drawn after a 12-hour fasting period for complete hepatology evaluation and to rule out other causes of liver disease.

### *Radiologic Examinations*

*Ultrasound and acoustic radiation force impulse elastography techniques*—All patients underwent B-mode and color Doppler ultrasound followed by liver ARFI elastography (Acuson S2000TM, Siemens Healthcare). The examinations were performed by an attending sonographer with 30 years of experience in US and 5 years of experience in ARFI elastography. The patients were instructed to fast for at least 6 hours before the examinations.

The following imaging findings were assessed: presence of hepatic nodule and, if present, the characteristics of the nodules on B-mode and color Doppler US, including diameter, location, echogenicity, and presence of Doppler signal. ARFI elastography was performed in a standardized manner (Appendix 1).

*CT technique*—Upper abdominal CT examinations were done in all patients without contraindications to iodine (44 patients), using a standardized protocol (Appendix 2) on a 64-MDCT scanner (Brilliance, Philips Healthcare; or Discovery HD 750, GE Healthcare). Patients fasted for at least 4 hours before the examination.

*MRI technique*—MRI was performed in patients without contraindications (48 patients) using a 3-T MRI unit (Achieva, Philips Healthcare) and a 16-channel phased-array receiver coil using a standard protocol (Appendix 3). Patients fasted for at least 4 hours before the examination. The liver images were acquired before and after IV injection of 0.1 mL/kg of gadoxetic acid (Primovist, Bayer Schering Pharma) at a rate of 2 mL/s using a power injector, followed by a 20-mL saline flush.

### *Image Analysis*

Two board-certificated abdominal radiologists specializing in abdominal imaging (with 12 and 3 years of experience) reviewed the CT and MRI studies separately, with a 1-month interval, and reached a consensus in all cases. The radiologists were aware of each patient's history of a Fontan procedure but were blinded to other clinical, laboratory, and ultrasound findings.

The radiologists analyzed the CT and MR images for the presence of hepatic nodules, with their imaging characteristics, and small hypervascular enhancing lesions on the arterial phase, characterized as focal hepatic lesion measuring less than 1.0 cm and detected only in the arterial phase. The Liver Reporting and Data System version 2017 descriptors were assessed, including arterial phase enhancement, capsule, washout, mosaic architecture, focal scar, and so on; however, the final category was not assigned, given that the system is not applied to patients with cirrhosis due to vascular disorders [27].

### *Statistical Analysis*

The continuous variables were summarized by using mean (± SD), and the categoric variables were expressed as counts and proportions. Intertest agreement was assessed by using weighted Cohen kappa values. Kappa values were interpreted qualitatively as follows: 0.00–0.20, slight agreement; 0.21–0.40, fair agreement; 0.41–0.60, moderate agreement; 0.61–0.80, substantial agreement; and 0.81–1.00, almost perfect agreement.

Hepatic nodules were correlated with the clinical, laboratory, and radiologic data. The dependence of hepatic nodule with the variables was performed using the *t* test or ANOVA for independent continuous variables without normal distribution, and the chi-square test or Fisher test was performed for categoric variables. Multivariate logistic regression was also used if association was detected at univariate analysis. ROC curve analysis was performed and the AUC was calculated to determine the diagnostic accuracy of liver stiffness on ARFI to predict hepatic nodule. The optimal threshold of liver stiffness was determined using ROC curve analysis followed by the Youden index.

For all statistical analyses, a $p < 0.05$ was considered statistically significant. The data were analyzed by using the statistical program software SPSS (version 22.0, IBM). The statistical methods of this study were reviewed by a statistician.

## Results

### *Patient Characteristics and Cardiologic, Hepatologic, and Laboratory Data*

There were 49 enrolled patients; 28 (57.1%) were women and the mean age was 26.2 ± 7 years. Two patients complained about ascites; otherwise, all patients had no symptoms. One patient had newly diagnosed hepatitis C,

one patient had celiac disease, and none of the patients had abnormal levels of α-fetoprotein. Two of the 49 patients (4.1%) underwent heart transplant, 3 and 6 years before the evaluation in the study. The other clinical and laboratory data are summarized in Table 1.

### *Radiologic Findings*

Hepatic nodules were detected in three of 49 (6.1%) patients at US, 14 of 44 patients (31.8%) at CT, and 19 of 48 patients (39.6%) at MRI, and none of them measured more than 3.0 cm. CT detected 33 hepatic nodules, and all nodules were found at MRI. Among the eight hepatic nodules that were solely detected at MRI, one was in a patient who did not undergo CT because of iodine allergy, and the remaining seven were detected only in the hepatobiliary phase at MRI. All nodules were well defined, and none of the patients with hepatic nodules presented with vascular thrombosis.

The characteristics of the hepatic nodules at US, CT, and MRI are summarized in Table 2. None of the nodules had capsule, restriction at DWI, or any other ancillary features that may favor malignancy.

Small hypervascular enhancing lesions were detected in 21 of 44 (47.7%) patients at CT and 25 of 48 (52.1%) patients at MRI. Figure 2 illustrates a representative case of a patient after Fontan procedure with hepatic nodule and small hypervascular enhancing lesions.

### *Ultrasound, CT, and MRI Agreement*

Table 3 summarizes the agreement between US, CT, and MRI in detecting hepatic nodules and small hypervascular enhancing lesions.

### *Correlations*

Regarding hepatic nodule, on univariate analysis, sex was statistically different between the groups, but on multivariate analysis this correlation was not maintained. Among the remaining clinical and laboratory variables, there was no significant difference between patients with and without hepatic nodules, including time since Fontan procedure (Table 1).

With regard to liver stiffness, the mean shear-wave propagation velocities at ARFI elastography were significantly higher in patients with hepatic nodules than in patients without nodules (2.64 ± 0.81 m/s vs 1.94 ± 0.49 m/s; $p = 0.002$) and significantly lower in patients who had received a heart transplant than in patients who had not (0.93 ± 0.15 m/s vs 2.28 ± 0.67 m/s; $p = 0.002$) (Fig. 3). Shear-wave propagation velocity at ARFI elastography was a significant predictor of presence of hepatic nodule, with an AUC of 0.767 ($p = 0.002$) (Fig. 4). We also found that, by using a cutoff of 2.0 m/s or higher on ARFI, the sensitivity and specificity in predicting hepatic nodule were 78.9% and 67.9%, respectively. There was no significant difference in liver stiffness according to the clinical and laboratorial variables.

## Discussion

In our study population, which was mostly composed of patients without symptoms (95.9%), we found that 6.1%, 31.8%, and 39.6% of patients had hepatic nodules seen at US, CT, and MRI, respectively, with an almost perfect agreement between CT and MRI and nonsignificant agreement between US and CT or MRI. We did not find any significant correlation between the presence of hepatic nodules and clinical or laboratory data, including time since Fontan procedure. In our study population, the liver stiffness values on ARFI elastography were significantly higher in patients with hepatic nodules and significantly lower in patients who had received a heart transplant. Furthermore, liver stiffness was a significant predictor of hepatic nodule (AUC, 0.767; $p = 0.002$) and using a cutoff of 2.0 m/s, the sensitivity and specificity in predicting hepatic nodule were 78.9% and 67.9%, respectively.

The frequencies of hepatic nodules at CT and MRI in our population are similar to or slightly higher than those of previous studies, which varied from 17% to 31% [10, 17, 28], possibly because we did liver-specific radiologic studies. On the other hand, the low frequency of hepatic nodules at US is similar to the results found by previous studies [29, 30]. Our results are also comparable with those presented by Bryant et al. [10] and Wallihan and Podberesky [31], who found no significant correlation between Fontan duration and presence of hepatic nodule.

Most of the hepatic nodules in our population had arterial hyperenhancement, and some of them showed washout. In patients who have undergone the Fontan procedure, benign nodules and HCC share similar imaging aspects (including arterial hyperenhancement and washout), comparable to patients with other vascular disorders, such as Budd-Chiari and chronic portal vein thrombosis [10, 14, 18, 32–34]. At MRI, most hepatic nodules in our population were hyperintense in the hepatobiliary phase (85.4%; 35/41). Increased contrast uptake in the hepatobiliary phase has been described in benign hepatic nodules [35]; however, some well-differentiated HCCs may exhibit hyperintensity and some adenomas can be hypointense [36]. Although our study was not designed to evaluate the nature of those hepatic nodules, considering the risk of HCCs [13, 14, 19, 20, 34] and the lack of specificity of imaging features, it seems to be reasonable to follow up these patients to detect early changes in imaging characteristics and, eventually, to indicate biopsy.

With regard to elastography, there are several studies that found a correlation between liver stiffness measured by different elastography imaging modalities with the total fibrosis score on liver biopsy in patients who have undergone the Fontan procedure [26, 34, 37, 38]. Our results are in line with those found by Melero-Ferrer et al. [26], who did not establish a correlation between time since Fontan procedure and liver stiffness at ARFI elastography. Conversely, our results are in contrast to those of previous studies using liver biopsy [39, 40] and different elastography imaging modalities, including FibroScan [37] and MR elastography [34], which found that increased liver fibrosis and liver stiffness, respectively, are correlated with time since Fontan procedure. These conflicting results may reflect that Fontan-related liver disease is multifactorial and do not depend exclusively on time interval since surgery.

On the other hand, we found that patients with hepatic nodules had significantly higher liver stiffness values, which was the only variable able to predict the presence of hepatic nodules. We speculate that higher values of liver stiffness may reflect a worse hepatic environment by both congestion and fibrosis, which are known risk factors for hepatic nodules. This finding may help with selecting patients who should be further imaged with CT or MRI. We also observed that liver stiffness was significantly lower in the two patients who underwent heart transplant. Despite the small number of patients, we hypothesize that the lower liver stiffness reflects an improvement in both congestion and fibrosis, because mild-to-moderate fibrosis can be reversible when the causal factor is removed [41].

Our results suggest that there is no clinical or laboratory finding reliable to exclude liver disease in this population, including time since Fontan procedure. Furthermore, a normal US is not able to rule out liver abnormalities, CT and MRI are similar to each other, and ARFI elastography may be helpful

**TABLE 1: Characteristics of the Patients With and Without Hepatic Nodules**

| Characteristic | All Patients (*n* = 49) | No Hepatic Nodules at MRI (*n* = 29) | Hepatic Nodules at MRI (*n* = 19) | *p*[a] | Normal Range | *p*[b] |
|---|---|---|---|---|---|---|
| Demographic data | | | | | | |
| Sex | | | | 0.049 | | 0.441 |
| Male | 21 (42.9) | 16 (76.2) | 5 (23.8) | | | |
| Female | 28 (57.1) | 13 (48.1) | 14 (51.9) | | | |
| Age (y), mean ± SD | 26.2 ± 7 | 25.9 ± 7.4 | 23.1 ± 7.4 | 0.783 | | |
| Body mass index, mean ± SD[c] | 22.3 ± 3.1 | 21.9 ± 3.0 | 22.8 ± 3.2 | 0.354 | | |
| Cardiologic data | | | | | | |
| Type of congenital heart disease | | | | 0.557 | | |
| Tricuspid atresia | 24 (48.9) | 12 (52.2) | 11 (47.8) | | | |
| Double outlet right ventricle | 6 (12.2) | 4 (66.7) | 2 (33.3) | | | |
| Double inlet left ventricle | 6 (12.2) | 5 (83.3) | 1 (16.7) | | | |
| Complex congenital heart diseases with functional single ventricle | 13 (26.5) | 8 (61.5) | 5 (38.5) | | | |
| Systemic ventricle morphologic features | | | | 0.903 | | |
| Left ventricle | 40 (81.6) | 23 (59.0) | 16 (41.0) | | | |
| Right ventricle | 4 (8.2) | 2 (50.0) | 2 (50.0) | | | |
| Bilateral ventricle | 3 (6.1) | 2 (66.7) | 1 (33.3) | | | |
| Unavailable | 2 (4.1) | | | | | |
| No. of surgeries[d] | | | | 0.949 | | |
| 1 | 8 (16.3) | 5 (62.5) | 3 (37.5) | | | |
| 2 | 7 (14.3) | 4 (57.1) | 3 (42.9) | | | |
| 3 | 25 (51.0) | 14 (56) | 11 (44.0) | | | |
| Age at Fontan procedure (y), mean ± SD | 11.3 ± 5.1 | 11.8 ± 5.1 | 10.1 ± 4.8 | 0.304 | | |
| Time from Fontan procedure to hepatology evaluation (y), mean ± SD | 14.8 ± 7.1 | 13.8 ± 7.0 | 15.8 ± 6.9 | 0.277 | | |
| Type of Fontan procedure | | | | 0.893 | | |
| Extracardiac conduit | 30 (61.2) | 18 (60.0) | 12 (40.0) | | | |
| Lateral tunnel | 13 (26.5) | 7 (53.8) | 6 (46.2) | | | |
| Atriopulmonary | 4 (8.2) | 2 (66.7) | 1 (33.1) | | | |
| Unavailable | 2 (4.1) | | | | | |
| Type of stage I palliation | | | | 0.79 | | |
| Blalock-Taussig anastomosis | 25 (51) | 14 (56.0) | 11 (44.0) | | | |
| Pulmonary artery bandage | 6 (12.2) | 3 (50.0) | 3 (50.0) | | | |
| None | 9 (18.4) | 6 (66.7) | 3 (33.3) | | | |
| Unavailable | 9 (18.4) | | | | | |
| Age at stage I palliation (y), mean ± SD | 1.3 ± 2.7 | 1.7 ± 3.4 | 0.79 ± 1.4 | 0.799 | | |
| Interval between Glenn and Fontan procedures (y), mean ± SD | 3.2 ± 3.2 | 3.6 ± 3.5 | 2.8 ± 2.9 | 0.648 | | |
| Presence of patent fenestration | | | | 0.231 | | |
| Yes | 12 (24.5) | 5 (41.7) | 7 (58.3) | | | |
| No | 30 (61.2) | 18 (62.1) | 11 (37.9) | | | |
| Unavailable | 7 (14.3) | | | | | |
| Heart transplant | 2 (4.1) | 2 (100) | 0 (0) | 0.512 | | |
| $O_2$ saturation[e] (%), mean ± SD | 93.9 ± 3.5 | 94.6 ± 2.7 | 92.8 ± 4.3 | 0.103 | | |

**(Table 1 continues on next page)**

**TABLE 1: Characteristics of the Patients With and Without Hepatic Nodules (continued)**

| Characteristic | All Patients (*n* = 49) | No Hepatic Nodules at MRI (*n* = 29) | Hepatic Nodules at MRI (*n* = 19) | *p*[a] | Normal Range | *p*[b] |
|---|---|---|---|---|---|---|
| Clinical and laboratory data | | | | 0.488 | | 0.158 |
| Splenomegaly | 7 (14.3) | 5 (71.4) | 2 (28.6) | | | |
| Ascites | 2 (4.1) | 0 (0) | 2 (100.0) | | | |
| Jaundice | 0 (0) | 0 (0) | 0 (0) | | | |
| Encephalopathy | 0 (0) | 0 (0) | 0 (0) | | | |
| Alcohol misuse | 8 (16.3) | 5 (62.5) | 3 (37.5) | 0.853 | | |
| Warfarin use | 37 (75.5) | 22 (61.1) | 14 (38.9) | 0.698 | | |
| Amiodarone use | 7 (14.3) | 4 (66.7) | 2 (33.3) | 0.705 | | |
| Platelet count (cells/mL/mm$^3$), mean ± SD | 195.3 ± 79.9 | 178.4 ± 60.5 | 225.4 ± 97.6 | 0.034 | 140–450 | 0.89 |
| Platelet count < 100,000 cells/mL/mm$^3$ | 2 (4.1) | 1 (50.0) | 1 (50.0) | 0.758 | 140–450 | |
| Platelet count < 150,000 cells/mL/mm$^3$ | 15 (30.6) | 10 (71.4) | 4 (28.6) | 0.317 | 140–450 | |
| INR, mean ± SD | | | | | | |
| Patients receiving warfarin | 2 ± 0.8 | 1.9 ± 0.81 | 2.3 ± 0.98 | 0.053 | 0.95–1.2 | |
| Patients not receiving warfarin | 1.1 ± 0.06 | 1.1 ± 0.07 | 1.1 ± 0.06 | 0.905 | 0.95–1.2 | |
| AST level (U/L), mean ± SD | 24.5 ± 8.8 | 23.7 ± 9.8 | 25.6 ± 7.2 | 0.131 | < 37 | |
| ALT level (U/L), mean ± SD | 26.1 ± 14.1 | 26.1 ± 16.1 | 26.5 ± 11.2 | 0.454 | < 41 | |
| GGT level (U/L), mean ± SD | 82.5 ± 53.6 | 87.0 ± 61.7 | 77.5 ± 40.2 | 1 | < 61 | |
| Alkaline phosphatase level (U/L), mean ± SD | 78.5 ± 23.4 | 77.3 ± 26.2 | 80.7 ± 19.6 | 0.316 | 40–129 | |
| Protein level (g/dL), mean ± SD | 7.2 ± 0.9 | 7.19 ± 0.8 | 7.28 ± 1.0 | 0.363 | 6.6–8.7 | |
| Albumin level (g/dL), mean ± SD | 4.5 ± 0.6 | 4.6 ± 0.5 | 4.38 ± 0.7 | 0.243 | 3.4–4.8 | |
| Total bilirubin level (mg/dL), mean ± SD | 0.9 ± 0.4 | 0.87 ± 0.38 | 0.90 ± 0.55 | 0.527 | 0.2–1.0 | |
| Direct bilirubin level (mg/dL), mean ± SD | 0.4 ± 0.2 | 0.38 ± 0.13 | 0.40 ± 0.20 | 0.816 | < 0.3 | |
| Alpha-fetoprotein level (ng/mL), mean ± SD | 2.9 ± 2.7 | 3.0 ± 3.2 | 2.8 ± 2.0 | 0.824 | < 10 | |
| AST-to-platelet ratio index, mean ± SD | 0.4 ± 0.2 | 0.43 ± 0.2 | 0.41 ± 0.35 | 0.417 | < 0.3 | |
| Model for end-stage liver disease excluding INR, mean ± SD | 9.7 ± 1.4 | 9.6 ± 1.2 | 9.9 ± 1.7 | 0.934 | < 11 | |
| Radiologic data | | | | | | |
| Ultrasound (*n* = 49) and ARFI elastography (*n* = 48) | | | | | | |
| Hepatic nodule | 3 (6.1) | | | | | |
| ARFI rate (m/s), mean ± SD | 2.2 ± 0.7 | 1.94 ± 0.49 | 2.64 ± 0.81 | 0.002 | | 0.006 |
| CT (*n* = 44) | | | | | | |
| Small hypervascular enhancing lesions on arterial phase | 21 (47.7) | 11 (55.0) | 9 (47.6) | 0.289 | | |
| Hepatic nodule | 14 (31.8) | | | | | |
| MRI (*n* = 48) | | | | | | |
| Small hypervascular enhancing lesions on arterial phase | 25 (52.1) | 14 (56.0) | 11 (44.0) | 0.514 | | |
| Hepatic nodule | 19 (39.6) | | | | | |

Note—Except where noted otherwise, data are number (percentage). INR = international normalized ratio, AST = aspartate aminotransferase, ALT = alanine aminotransferase, GGT = γ-glutamyltransferase, ARFI = acoustic radiation force impulse.

[a]Univariate analysis.

[b]Multivariate logistic regression (if significant variables on univariate analysis).

[c]Weight in kilograms divided by the square of height in meters.

[d]*n* = 40 cases.

[e]*n* = 35 cases.

**TABLE 2: Characteristics of the Hepatic Nodules on Ultrasound, CT, and MRI**

| Modality, Characteristic | Value |
|---|---|
| Ultrasound (*n* = 3) | |
| Diameter (mm), mean ± SD (range) | 1.3 ± 0.5 (1.1–2.0) |
| Echogenicity | |
| Hypoechogenic | 0 (0) |
| Isoechogenic | 0 (0) |
| Hyperechogenic | 3 (100) |
| CT (*n* = 33) | |
| Diameter (mm), mean ± SD (range) | 1.6 ± 0.5 (1.1–3.0) |
| Arterial hyperenhancement | 32 (96.9) |
| Washout appearance | 8 (24.2) |
| MRI (*n* = 41) | |
| Diameter (mm), mean ± SD (range) | 1.5 ± 0.5 (1.1–3.0) |
| T1-weighted imaging | |
| Hypointense | 0 (0) |
| Isointense | 39 (95.1) |
| Hyperintense | 2 (4.9) |
| T2-weighted imaging | |
| Hypointense | 3 (7.3) |
| Isointense | 38 (92.7) |
| Hyperintense | 0 (0) |
| Arterial hyperenhancement | 32 (78.0) |
| Washout appearance | 2 (4.9) |
| Hepatobiliary phase | |
| Hypointense | 1 (2.4) |
| Isointense | 5 (12.2) |
| Hyperintense | 35 (85.4) |

Note—Except where noted otherwise, data are number (percentage) of nodules.

**TABLE 3: Intertest Agreement of Ultrasound, CT, and MRI in Detecting Hepatic Nodules and Small Hypervascular Enhancing Lesions**

| Lesion, Modality | Ultrasound | | CT | |
|---|---|---|---|---|
| | κ | *p* | κ | *p* |
| Hepatic nodules | | | | |
| CT | 0.006 | 0.095 | | |
| MRI | 0.083 | 0.032 | 0.849 | < 0.001 |
| Small hypervascular enhancing lesions, MRI | | | 0.721 | < 0.001 |

Note—Overall agreement was 65.9% (95% CI, 50.1–79.5%).

in selecting patients after Fontan procedure for screening liver disorders. Finally, despite the small number of patients who underwent heart transplant, the significant lower levels of their liver stiffness may suggest that heart transplant alone can reduce hepatic damage.

There were some potential limitations in this study. First, there was no correlation with liver biopsy, which did not enable us to grade the liver fibrosis and to show the nature of the hepatic nodule. Furthermore, the heart transplant recipients were not evaluated before the transplantation. Therefore, further prospective studies are needed to overcome these limitations and to provide a better generalization of our results.

In our study population, more than one-third of patients who had undergone the Fontan procedure had hepatic nodules seen at CT or MRI, but US did not detect the majority of them. Liver stiffness at ARFI elastography was significantly higher in patients with hepatic nodule and significantly lower in the two patients after heart transplant. ARFI may help screening patients who should be further imaged with CT or MRI.

## Acknowledgments

We thank Valeria Lira for providing Figure 1A and Valdecir Marvulle for his statistical advice.

## References

1. Fontan F, Baudet E. Surgical repair of tricuspid atresia. *Thorax* 1971; 26:240–248
2. Jacobs JP, Maruszewski B. Functionally univentricular heart and the Fontan operation: lessons learned about patterns of practice and outcomes from the congenital heart surgery databases of the European association for cardio-thoracic surgery and the society of thoracic surgeons. *World J Pediatr Congenit Heart Surg* 2013; 4:349–355
3. Khairy P, Poirier N, Mercier LA. Univentricular heart. *Circulation* 2007; 115:800–812
4. Gewillig M. The Fontan circulation. *Heart* 2005; 91:839–846
5. Fontan F, Kirklin JW, Fernandez G, et al. Outcome after a "perfect" Fontan operation. *Circulation* 1990; 81:1520–1536
6. Khairy P, Fernandes SM, Mayer JE Jr, et al. Long-term survival, modes of death, and predictors of mortality in patients with Fontan surgery. *Circulation* 2008; 117:85–92
7. Ono M, Boethig D, Goerler H, Lange M, Westhoff-Bleck M, Breymann T. Clinical outcome of patients 20 years after Fontan operation: effect of fenestration on late morbidity. *Eur J Cardiothorac Surg* 2006; 30:923–929
8. Bradley E, Hendrickson B, Daniels C. Fontan liver disease: review of an emerging epidemic and management options. *Curr Treat Options Cardiovasc Med* 2015; 17:51
9. Rychik J, Veldtman G, Rand E, et al. The precarious state of the liver after a Fontan operation: summary of a multidisciplinary symposium. *Pediatr Cardiol* 2012; 33:1001–1012
10. Bryant T, Ahmad Z, Millward-Sadler H, et al. Arterialised hepatic nodules in the Fontan circulation: hepatico-cardiac interactions. *Int J Cardiol* 2011; 151:268–272
11. Eipel C, Abshagen K, Vollmar B. Regulation of hepatic blood flow: the hepatic arterial buffer response revisited. *World J Gastroenterol* 2010; 16:6046–6057
12. Guérin F, Wagner M, Liné A, et al. Hepatic proliferation and angiogenesis markers are increased after portal deprivation in rats: a study of molecular, histological and radiological changes. *PLoS One* 2015; 10:e0125493
13. Asrani SK, Warnes CA, Kamath PS. Hepatocel-

lular carcinoma after the Fontan procedure. *N Engl J Med* 2013; 368:1756–1757

14. Ewe SH, Tan JL. Hepatocellular carcinoma: a rare complication post Fontan operation. *Congenit Heart Dis* 2009; 4:103–106
15. Ghaferi AA, Hutchins GM. Progression of liver pathology in patients undergoing the Fontan procedure: chronic passive congestion, cardiac cirrhosis, hepatic adenoma, and hepatocellular carcinoma. *J Thorac Cardiovasc Surg* 2005; 129:1348–1352
16. Kendall TJ, Stedman B, Hacking N, et al. Hepatic fibrosis and cirrhosis in the Fontan circulation: a detailed morphological study. *J Clin Pathol* 2008; 61:504–508
17. Kiesewetter CH, Sheron N, Vettukattill JJ, et al. Hepatic changes in the failing Fontan circulation. *Heart* 2007; 93:579–584
18. Kwon S, Scovel L, Yeh M, et al. Surgical management of hepatocellular carcinoma after Fontan procedure. *J Gastrointest Oncol* 2015; 6:E55–E60
19. Takuma Y, Fukada Y, Iwadou S, et al. Surgical resection for hepatocellular carcinoma with cardiac cirrhosis after the Fontan procedure. *Intern Med* 2016; 55:3265–3272
20. Oh C, Youn JK, Han JW, Kim GB, Kim HY, Jung SE. Hepatocellular carcinoma after the Fontan procedure in a 16-year-old girl: a case report. *Medicine (Baltimore)* 2016; 95:e4823
21. Bhatt AB, Foster E, Kuehl K, et al. Congenital heart disease in the older adult: a scientific statement from the American Heart Association. *Circulation* 2015; 131:1884–1931
22. Silversides CK, Salehian O, Oechslin E, et al. Canadian Cardiovascular Society 2009 Consensus Conference on the management of adults with congenital heart disease: complex congenital cardiac lesions. *Can J Cardiol* 2010; 26:e98–e117
23. Daniels CJ, Bradley EA, Landzberg MJ, et al. Fontan-associated liver disease: proceedings from the American College of Cardiology stakeholders meeting, October 1 to 2, 2015, Washington DC. *J Am Coll Cardiol* 2017; 70:3173–3194
24. Baumgartner H, Bonhoeffer P, De Groot NM, et al. ESC guidelines for the management of grown-up congenital heart disease (new version 2010). *Eur Heart J* 2010; 31:2915–2957
25. Rockey DC, Caldwell SH, Goodman ZD, Nelson RC, Smith AD; American Association for the Study of Liver Diseases. Liver biopsy. *Hepatology* 2009; 49:1017–1044
26. Melero-Ferrer JL, Osa-Sáez A, Buendía-Fuentes F, et al. Fontan circulation in adult patients: acoustic radiation force impulse elastography as a useful tool for liver assessment. *World J Pediatr Congenit Heart Surg* 2014; 5:365–371
27. Elsayes KM, Hooker JC, Agrons MM, et al. 2017 Version of LI-RADS for CT and MR imaging: an update. *RadioGraphics* 2017; 37:1994–2017
28. Bulut OP, Romero R, Mahle WT, et al. Magnetic resonance imaging identifies unsuspected liver abnormalities in patients after the Fontan procedure. *J Pediatr* 2013; 163:201–206
29. Camposilvan S, Milanesi O, Stellin G, Pettenazzo A, Zancan L, D'Antiga L. Liver and cardiac function in the long term after Fontan operation. *Ann Thorac Surg* 2008; 86:177–182
30. Yoo BW, Choi JY, Eun LY, Park HK, Park YH, Kim SU. Congestive hepatopathy after Fontan operation and related factors assessed by transient elastography. *J Thorac Cardiovasc Surg* 2014; 148:1498–1505
31. Wallihan DB, Podberesky DJ. Hepatic pathology after Fontan palliation: spectrum of imaging findings. *Pediatr Radiol* 2013; 43:330–338
32. Babaoglu K, Binnetoglu FK, Aydogan A, et al. Hepatic adenomatosis in a 7-year-old child treated earlier with a Fontan procedure. *Pediatr Cardiol* 2010; 31:861–864
33. Valla DC. Budd-Chiari syndrome/hepatic venous outflow tract obstruction. *Hepatol Int* 2018; 12(suppl 1):168–180
34. Poterucha JT, Johnson JN, Qureshi MY, et al. Magnetic resonance elastography: a novel technique for the detection of hepatic fibrosis and hepatocellular carcinoma after the Fontan operation. *Mayo Clin Proc* 2015; 90:882–894
35. Seale MK, Catalano OA, Saini S, Hahn PF, Sahani DV. Hepatobiliary-specific MR contrast agents: role in imaging the liver and biliary tree. *RadioGraphics* 2009; 29:1725–1748
36. Huppertz A, Haraida S, Kraus A, et al. Enhancement of focal liver lesions at gadoxetic acid-enhanced MR imaging: correlation with histopathologic findings and spiral CT—initial observations. *Radiology* 2005; 234:468–478
37. Friedrich-Rust M, Koch C, Rentzsch A, et al. Noninvasive assessment of liver fibrosis in patients with Fontan circulation using transient elastography and biochemical fibrosis markers. *J Thorac Cardiovasc Surg* 2008; 135:560–567
38. Kutty SS, Peng QH, Danford DA, et al. Increased hepatic stiffness as consequence of high hepatic afterload in the Fontan circulation: a vascular Doppler and elastography study. *Hepatology* 2014; 59:251–260
39. Surrey LF, Russo P, Rychik J, et al. Prevalence and characterization of fibrosis in surveillance liver biopsies of patients with Fontan circulation. *Hum Pathol* 2016; 57:106–115
40. Maisey NR, Webb A, Flux GD, et al. FDG-PET in the prediction of survival of patients with cancer of the pancreas: a pilot study. *Br J Cancer* 2000; 83:287–293
41. Pellicoro A, Ramachandran P, Iredale JP. Reversibility of liver fibrosis. *Fibrogenesis Tissue Repair* 2012; 5(suppl 1):S26

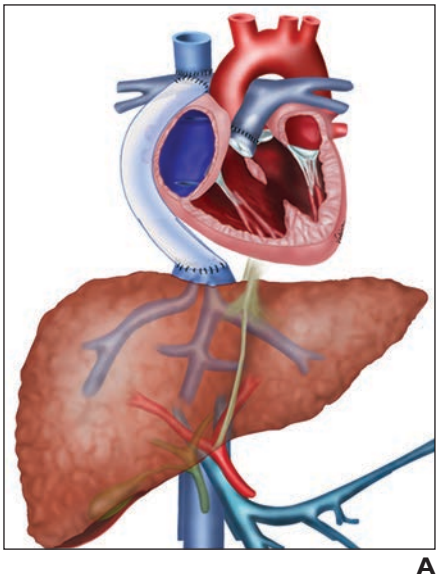

A

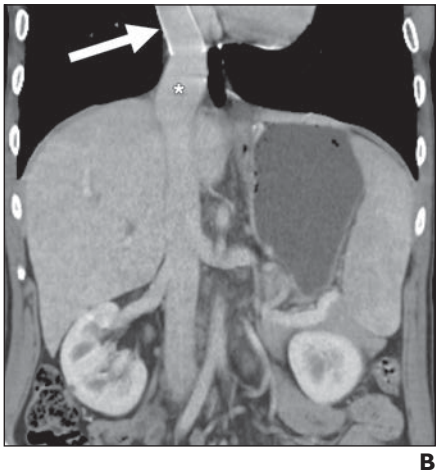

B

**Fig. 1**—Single ventricle and Fontan technique.
**A,** Illustration shows extracardiac Fontan technique in patient with single ventricle and hepatic consequences. (Illustration by Lira V)
**B,** 19-year-old woman with single ventricle. Contrast-enhanced CT in coronal plane shows extracardiac conduit (*arrow*) causing dilatation of inferior vena cava (*asterisk*), which leads to hepatomegaly and heterogeneous enhancement of liver parenchyma.

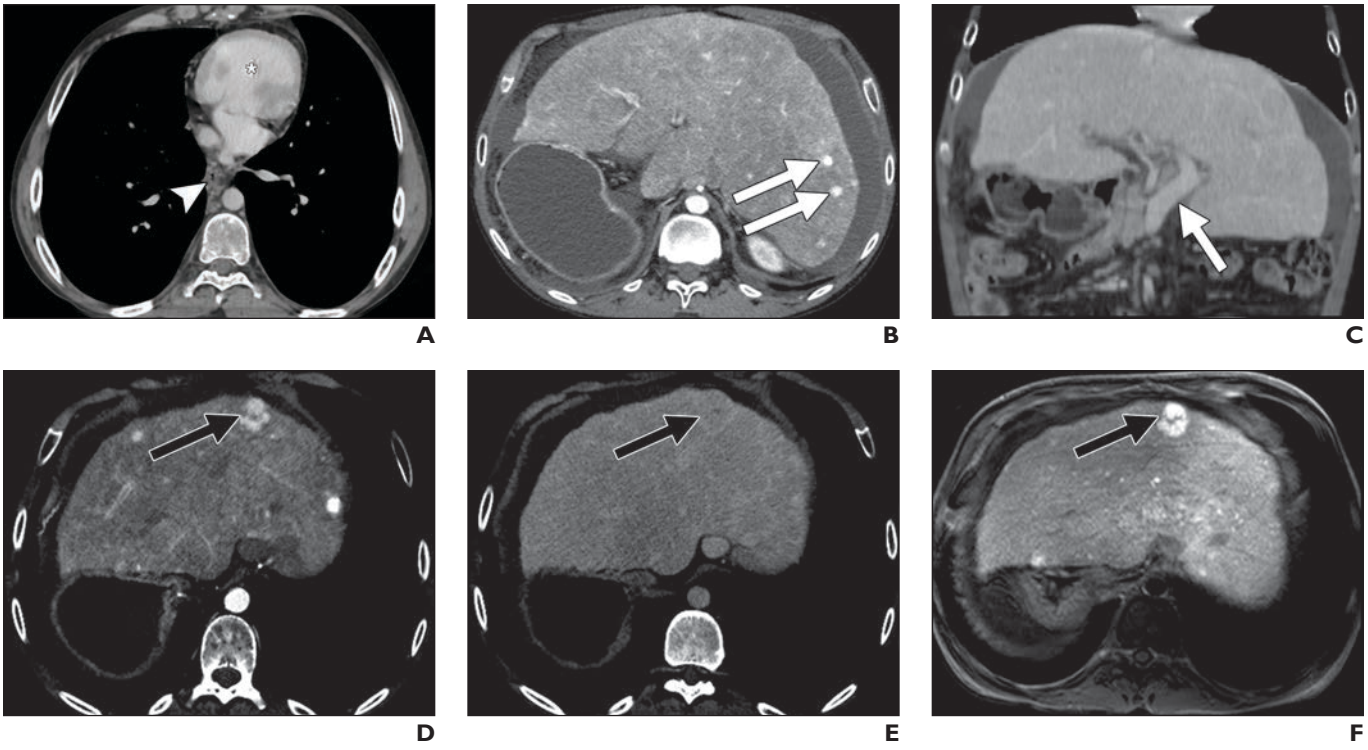


**Fig. 2**—25-year-old man with single ventricle, abdominal situs inversus, and asplenia who had hepatic nodule and small hypervascular enhancing lesions scattered in liver parenchyma and underwent Fontan procedure.
**A,** Contrast-enhanced CT (CECT) of thoracoabdominal transition shows single ventricle (*asterisk*) and periesophageal varices (*arrowhead*).
**B** and **C,** CECT images in axial (**B**) and coronal (**C**) planes show hepatomegaly, liver nodularity, small hypervascular enhancing lesions (*arrows*, **B**), ascites, and enlargement of portal vein (*arrow*, **C**).
**D**–**F,** MR images show that patient also had hepatic nodules, and biggest one (*arrows*) was hypervascular on arterial phase (**D**), had washout appearance on portal phase (**E**), and had increased uptake in hepatobiliary phase (**F**).

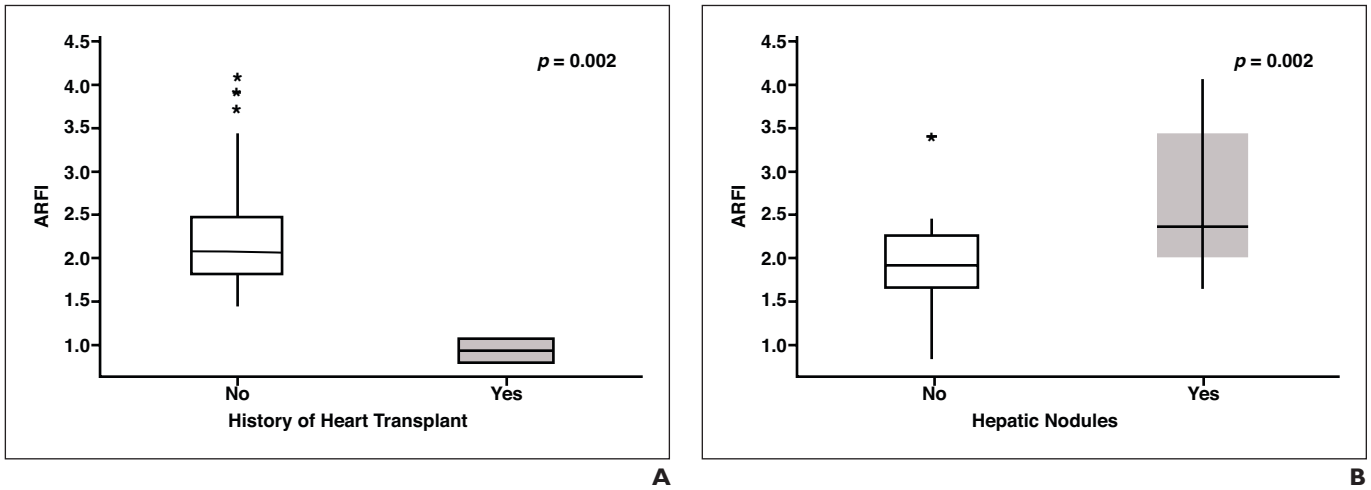


**Fig. 3**—Mean liver stiffness measured on acoustic radiation force impulse (ARFI) elastography.
**A** and **B,** Box plots show liver stiffness in patients with and without previous heart transplant (**A**) and in patients with and without hepatic nodules (**B**). Vertical lines denote 95% CIs, and asterisks denote outliers.

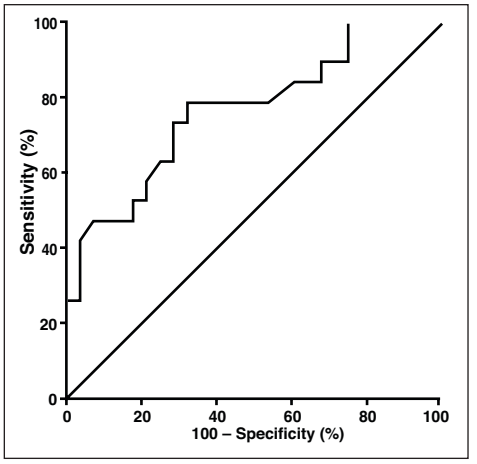


**Fig. 4**—ROC curve of liver stiffness on acoustic radiation force impulse elastography as predictor of hepatic nodule.

## APPENDIX 1: Acoustic Radiation Force Impulse Elastography Protocol

Acoustic radiation force impulse elastography was performed with the patient lying in the dorsal decubitus position with the right arm in maximal abduction; imaging was performed of the right lobe of the liver, through the intercostal spaces. The measurements were obtained with assistance by a real-time B-mode ultrasound image. The ROI used to measure the shear-wave propagation velocity was in the right hepatic lobe, 15 mm below the liver capsule, with a maximum thickness of 8 cm, and far from large vascular structures and the gallbladder. Ten valid measurements (meters per second) were obtained for each patient. The median value was determined as the representative measurement. Unreliable results were defined as an interquartile range ratio greater than 30%.

## APPENDIX 2: CT Protocol

CT was performed using the following scanning parameters: maximum of 300 mA (varying according to the patient's weight), 120 kVp, 0.8-second tube rotation time, and pitch of 1.375/1 mm/rotation. Images were acquired before and after IV injection of 1.5 mL/kg of iodinated contrast agent (iopromide; Ultravist, Bayer Schering Pharma), at a rate of 4 mL/s using a power injector, followed by a 25-mL saline flush. Bolus-tracking software was used to trigger the arterial phase scans at 15 seconds after contrast enhancement of the upper abdominal aorta to an attenuation threshold of 150 HU. The portal venous and delayed phases started at a fixed delay of 60 and 90 seconds, respectively, after the contrast agent injection.

## APPENDIX 3: MRI Protocol

The MRI protocols were performed with standard sequences, including respiratory-triggered axial T2-weighted fat- and non–fat-suppressed images, coronal single-shot T2-weighted images, axial T1-weighted in- and opposed-phase images, and axial DW images with b values of 0, 100, and 700 s/mm2. Unenhanced, arterial phase (20 seconds), portal phase (60 seconds), late phase (90 seconds), and 20-minute delayed hepatobiliary phase images were obtained using a T1-weighted 3D turbo field-echo sequence (T1-weighted high-resolution isotropic volume examination; THRIVE, Philips Healthcare) with spectral attenuated inversion recovery fat suppression. DWI sequences were performed before the administration of gadoxetic acid, and the timing for the arterial phase imaging was determined using MR fluoroscopic bolus detection.